

Potential and Limitations of Battery-Powered All-Electric Regional Flights— A Norwegian Case Study

Trym Bærheim, Jacob J. Lamb¹, Jonas Kristiansen Nøland², *Senior Member, IEEE*, and Odne S. Burheim

Abstract—The purpose of this study is to look at both the potential and the limitations of first-generation electric aviation technology while emphasizing Norway’s geographical opportunities and unique regional network. Electric flight distances of up to 400 km would cover around 77% of all flights within Norway. Currently, there is limited research into the suitability of battery-powered all-electric aviation in such scenarios, where Norway is an ideal case study location. In this work, the key factors, including battery technologies, propulsion systems, aircraft designs, and important aspects of the flight profile, are investigated to determine the suitability of specific routes in terms of the required power, energy, and battery size. A case study of five different flight distances in Norway (77–392 km) and two different aircraft bodies (one retrofitted with an electric powertrain and one completely designed around the electric drivetrain) is presented. While the completely redesigned aircraft is observed to fulfill the power requirements of the routes, the results suggest that modest energy density improvements in batteries would facilitate retrofitting preexisting aircraft. Finally, the study shows that it will be feasible to operate small (9–39 passengers) electric aircraft on short-haul flights in Norway through either new aircraft designs or retrofitting shortly.

Index Terms—Battery–electric aircraft, electric propulsion, mission profile modeling, motion modeling, regional flights.

NOMENCLATURE

Δt_{res}	Total reserve cruising time to diversion airport [s] or [min].
η_{gear} and η_{prop}	Efficiency of gear and propeller [%].
η_{pec} and η_{mot}	Efficiency of power electronics converter and electric motor [%].
η_{tot}	Total efficiency of propulsion system [%].
$\text{SOC}_{\text{final}}$ and SOC_{min}	Final and minimum state of charge of battery for a given mission profile [%].

Manuscript received 11 March 2022; revised 3 July 2022; accepted 15 August 2022. Date of publication 18 August 2022; date of current version 21 February 2023. The work of Jacob J. Lamb and Odne S. Burheim was supported by the ENERSENSE Research Initiative at the Norwegian University of Science and Technology (NTNU). The work of Jonas Kristiansen Nøland was supported by the Local NTNU Clean Aviation Initiative. (*Corresponding author: Jacob J. Lamb.*)

Trym Bærheim, Jacob J. Lamb, and Odne S. Burheim are with the Department of Energy and Process Engineering, Norwegian University of Science and Technology, 7034 Trondheim, Norway (e-mail: jacob.j.lamb@ntnu.no).

Jonas Kristiansen Nøland is with the Department of Electric Power Engineering, Norwegian University of Science and Technology, 7034 Trondheim, Norway.

This article has supplementary downloadable material available at <https://doi.org/10.1109/TTE.2022.3200089>, provided by the authors.

Digital Object Identifier 10.1109/TTE.2022.3200089

μ	Rolling friction coefficient (CRF).
ρ	Mass density of air [kg/m^3].
θ and θ_{cruise}	Aircraft’s instantaneous and cruising flight path angle, respectively [$^\circ$] or [rad].
a and g	Acceleration of aircraft and acceleration of gravity [m/s^2].
C_D	Drag coefficient of aircraft.
e_{bat}	Battery’s gravimetric energy density metric [Wh/kg] or [kWh/kg].
E_{bat} , E_{peak} , and E_{res}	Battery’s maximum available energy content, peak energy use, and reserves [kWh] or [MJ].
$E_{T\infty}$, E_{acc} , and E_{aux}	Energy needed for cruising, acceleration and deceleration, and auxiliary functions [kWh] or [MJ].
F , L , A , D , and D_w	Aircraft’s thrust, lift, lift constant, drag, and wind force, respectively [N].
F_f , W , and N	Friction force, weight, and normal force, respectively [N].
h and h_{cruise}	Altitude in a generic sense and cruising altitude of mission profile [m] or [km].
k_{bat}	Battery’s utilization factor.
m , m_{bat} , and m_{tot}	Mass in a generic sense, battery mass, and aircraft total mass [kg].
P and P_{bat}	Aircraft’s traction power and battery power [kW] or [MW].
R	Range of aircraft [m] or [km].
S	Frontal surface area of the aircraft [m^2].
t_{descend} and t_{flight}	Time to descend and flight is completed, respectively [s] or [min].
t_{takeoff} , t_{climb} , and t_{cruise}	Time to takeoff, climb, and cruise is completed, respectively [s] or [min].
v , v_{cruise} , and v_{takeoff}	Airplane’s instantaneous, cruise, and takeoff speed [m/s] or [km/h].

I. INTRODUCTION

EUROPE’S aviation sector emitted 192 million tons of CO_2 in 2019, which is 13.9% of transport GHG emission, second only to road transport [1]. Even though the effect of COVID-19 in 2020 led to an emission reduction of 57% in

Europe due to travel restrictions [2], there has been a steady growth in global air traffic of roughly 4%–8% per year since 2010 [3]. There is still a significant risk that the overall CO₂ emissions from aviation will triple by 2050 should no major action be taken, as the growth inevitably leads to an increase in emission from fuel burn with 80% of aviation emissions coming from long-distance flights over 1500 km [4]. To reach the Paris Agreement from 2015 [5], action must be taken in all areas of society, including the transportation sector. While Norway is presently adopting technological advances in both the automotive and marine sectors (e.g., e-buses and e-ferries), there is no electric option for commercial aviation. However, the possibility of aircraft electrification is becoming appealing. The Norwegian airline, Widerøe, which is the largest actor in the regional segment in Scandinavia, is envisioning an all-electric aircraft in the commuter market by 2026 [6]. They have joint forces with Rolls-Royce and Airframer Tecnam to retrofit a preexisting aircraft that is already certified. Although the structure is not optimized for the electric power train, it is assumed to have a faster technical track to commercialization. Still, there are many challenges to be faced with implementing electric propulsion systems in aviation. These challenges include reducing the weight and increasing the energy density and lifetime of the batteries while still achieving the desired distances and complying with the strict safety regulations present in this sector. In earlier engineering efforts, electrification of auxiliary energy needs and partially electrified propulsion (such as more-electric and hybrid-electric solutions) have been pursued [7], [8], [9], [10], [11], [12]. However, these solutions will not have a large climate impact, and battery-powered all-electric aviation is seen as more promising.

To scale up electric propulsion systems in aviation, reliability, efficiency, and specific power density are considered the key figures of merit [13]. Still, weight is the major technological barrier [14], which includes all components of the propulsion system. However, for battery-powered propulsion, the specific energy density of the energy storage and the mass of the battery is the main barrier to electrification, as it will be the major contributor to the overall weight [15]. Even though there is a need to establish certifiable aerospace-grade electrical components for aviation, the technical path to develop these components is promising [16]. Already, all-electric battery-powered aircraft are well suited to urban air mobility (UAM) applications and in the commuter flight segment [17]. The question is whether and to what extent batteries could be scaled up to power regional flights as well, which will be addressed in this article.

In conventional studies that predict the potential for electric aircraft, a simplified form of the range equation is considered (i.e., the modified Breguet equation) [13], [15], [18], which overlooks the details of several of the phases of the mission profile, including takeoff, acceleration, and climbing. However, the cruising phase is only a fraction of the overall mission profile for regional flights, which makes the overall prediction for energy requirements inaccurate. Moreover, an accurate physical model that takes the realistic mission profile from actual flight data into account can provide detailed estimates

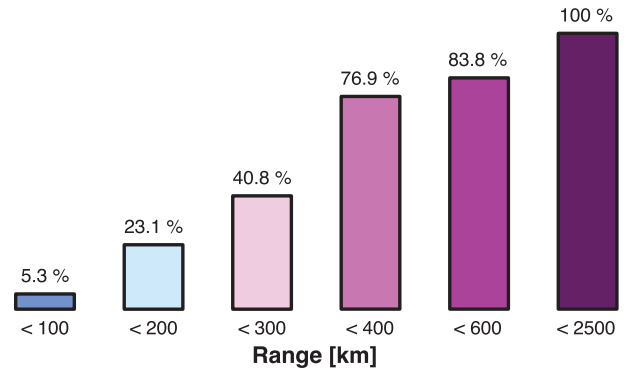


Fig. 1. Accumulative distribution of domestic flights in Norway with more than 100 departures in 2019 by distance [19].

for the needed peak power. Therefore, this work develops a framework from first principles to deal with the shortcomings of earlier studies of battery-powered aviation and uses the detailed model to make predictions on five Norwegian regional flight routes based on real-world mission profile data.

This study describes the opportunities for electric aviation on domestic routes within Norway by using five current routes' flight-plan data as a case study (routes between 77 and 392 km). Two aircraft frames are assessed within this study: 1) the De Havilland Canada Dash 8-100 (DHC-100) aircraft that is currently used, with a retrofitted electric powertrain and 2) the Eviation Alice that is a purpose-built electric aircraft currently being developed. These aircraft can carry up to 39 and nine passengers, respectively. The required battery power and capacity are determined through the aircraft's physical parameters (e.g., weight and drag) and the climate rate required for the specific routes (essential for safe flight through the abrupt mountainous terrain of Norway). This also takes into account the weight of the battery, as this will be a considerable contribution to the entire aircraft's weight. The theoretical aircraft are then optimized for specific energy capacity, efficiency, lift-to-drag ratio, and mass in order to fulfill the requirements of the five separate routes. This results in insight into the required battery power and capacity for the separate routes, as well as the battery-to-aircraft mass ratio considering different battery energy capacities.

II. DOMESTIC FLIGHTS IN NORWAY

In the first quarter of 2021 alone, there were more than 1 240 000 passengers using domestic air transportation in Norway [19]. Norway has a unique opportunity to be a pioneer in aviation electrification due to the following reasons:

- 1) easy access to renewable energy sources;
- 2) industrial expansion of battery production;
- 3) an extensive grid of domestic airports with frequent departures and limited alternative means of transportation;
- 4) willingness for change from industrial actors in the aviation sector.

A. Current Aircraft Fleet

The three major airlines operating in Norway are Widerøe, SAS, and Norwegian. The capacity and range of the smallest planes in each fleet are summarized in Table I.

TABLE I
SMALLEST AIRCRAFT IN THE FLEET OF MAJOR NORWEGIAN AIRLINES

Airline	Smallest aircraft	Range	Passengers (PAX)	Portion of fleet	Share
SAS	ATR-72-600	930 km	70	9/164	5.5 %
Norwegian	Boeing 737-800	5436 km	186-189	85/140	60.7 %
Widerøe	Dash 8-100	1796 km	39	23/45	51.1 %

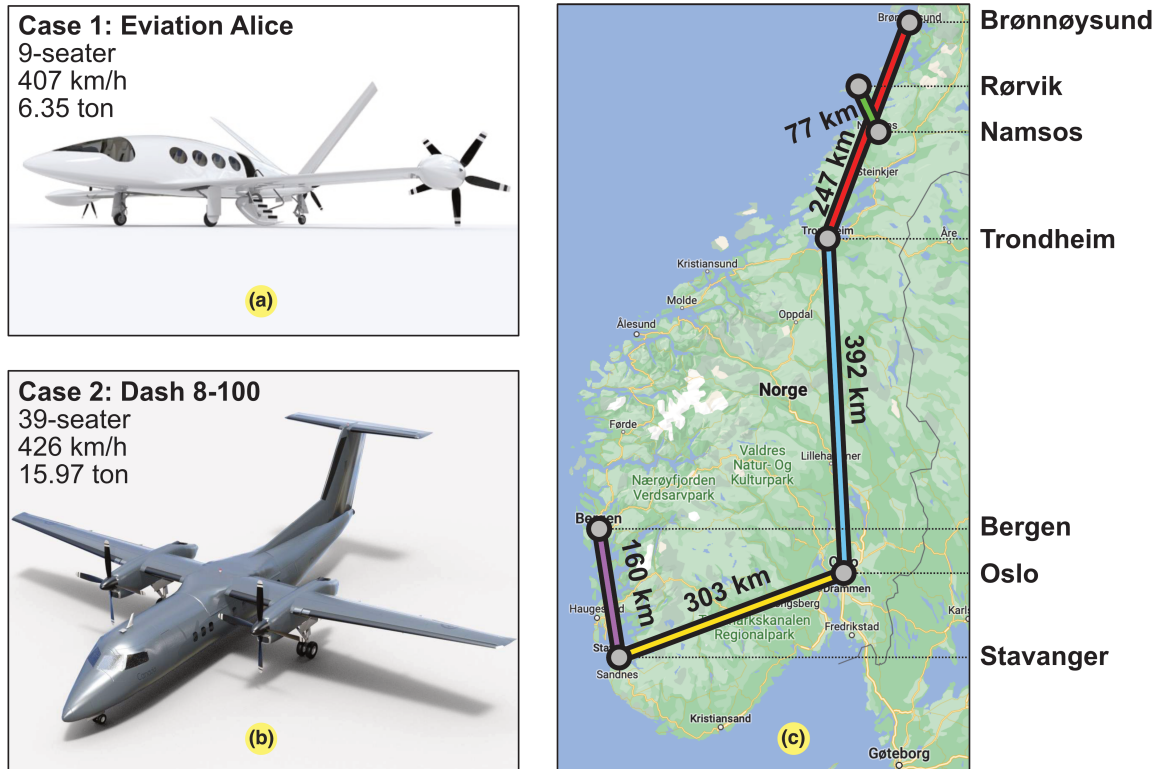


Fig. 2. Overview of the conducted Norwegian case study. (a) Case 1: Eviation Alice [24]. (b) Case 2: DHC-100 [25]. (c) Map depicting the five handpicked routes considered in the regional study.

B. Benefits of Norwegian Energy Generation

Electric aviation would have an advantage over traditional aircraft in terms of GHG emissions if the energy used to charge the batteries is renewable [15]. Norway has a high share of renewable energy sources and, therefore, has the potential for much cleaner flights than many other countries [20]. In addition, by exploiting the available renewable energy, the goal is to produce batteries with a much lower CO₂ footprint than what is being done in existing factories [21].

C. Advantageous Norwegian Landscape

Norway has many short-distance routes and commuter aircraft, with few passengers per plane and few alternative means of transportation due to the challenging terrain. This is ideal for the early implementation of electric aircraft for the two following reasons.

- 1) The smallest electric aircraft produces the largest benefits in terms of emissions and cost reduction compared to traditional aircraft [22].
- 2) The specific energy of state-of-the-art (SotA) batteries would not be capable of carrying a large aircraft with many passengers [22].

The necessity of airborne transport is driven by Norway's geography, which is characterized by long coasts and mountainous terrain (i.e., air transport is often the only possible way to travel).

D. Political, Social, and Industrial Drivers

An overview of air traffic between the airports in Norway has been made based on numbers from SSB. The accumulative distribution of the most frequently used flight paths (determined by having more than 100 flights per year) is shown in Fig. 1. Around 77% of the domestic flights with over 100 departures per year flew a distance shorter than 400 km.

With the advantages mentioned above, including a large network of relatively short and frequent flights, easy access to clean energy sources, and a political and social drive for making transportation greener, Norway has a clear potential for being a pioneer in first-generation electric aviation.

E. Selected Case Study

This article focuses on the challenges that must be overcome to make fully electric flight possible. Factors limiting the

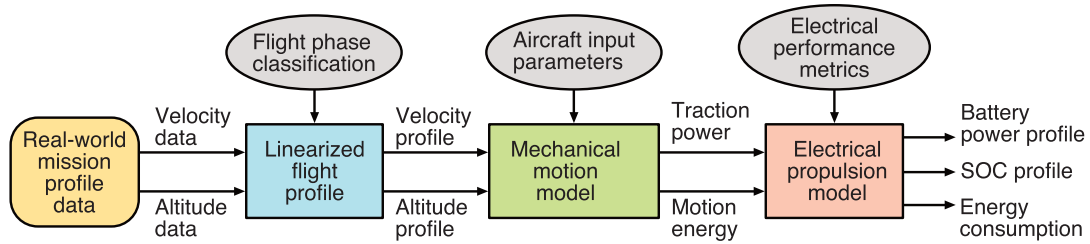


Fig. 3. Overview of the prediction model proposed in this article.

TABLE II

CASE 1: ELECTRIC AIRCRAFT ALICE'S KEY SPECIFICATIONS [24], WHERE THE L/D RATIO WAS ESTIMATED

Maximum speed	463 km/h
Cruising speed	407 km/h
Cruising altitude	3.048 km
Take-off field length	0.914 km
Maximum range (incl. 45 min reserve)	815 km
Maximum take-off weight (MTOW)	6350 kg
Maximum payload	1134 kg
Battery weight	3600 kg
Peak propulsion power	900 kW
Cruising propulsion power	260 kW
Battery's energy storage (NMC chemistry)	920 kWh
Lift-to-drag ratio (L/D)	20
Number of passengers (PAX)	9

TABLE III

CASE 2: SPECIFICATION OF DHC-100 [25]

Maximum speed	482 km/h
Cruising speed [26]	426 km/h
Take-off speed [26]	176 km/h
Maximum take-off weight (MTOW)	15 966 kg
Maximum payload	3606 kg
Lift-to-drag ratio (L/D) [27], [28]	15
Number of passengers (PAX)	39

range of an electric aircraft are presented and discussed, and a case study of electric flight in Norway is conducted, considering two aircraft bodies and five routes (see Fig. 2). Two of these handpicked routes (i.e., Oslo–Trondheim and Oslo–Stavanger) are among Europe's busiest domestic flight routes [23].

Moreover, the two aircraft chosen for this work are given as follows.

- 1) The largest electric aircraft in development is Eviation's Alice [see Fig. 2(a)]. Since it is not a retrofit, it can take advantage of the opportunities to improve aerodynamics (e.g., higher L/D ratio).
- 2) The smallest aircraft in Widerøe's fleet (DHC-100) is considered through a retrofitting strategy [see Fig. 2(b)].

In addition to the aircraft bodies, five flight distances were studied [see Fig. 2(c)]. These distances are based on actual flights that are carried out in Norway today [19].

III. METHODOLOGY AND ASSUMPTIONS

This section focuses on establishing the methodology for the handpicked case studies. An overall sketch of the framework is depicted in Fig. 3, where each part is described in the subsections hereafter.

A. Aircraft Physical Model From Input Data

To estimate the energy required for different missions, the properties of the aircraft must be given. Specifically, using equations derived in the Supplementary Material, the aerodynamic lift-to-drag (L/D) ratio and the total weight are required. Table II presents the parameters that are given on the Eviation's website [24] of their aircraft Alice. The DHC-100 aircraft's key performance data are given in Table III.

B. Calculation Assumptions

The following assumptions have been made for the general parametric analysis.

- 1) To estimate the rolling friction (F_f) when the aircraft is at ground level, a coefficient of rolling friction (CRF) is used, where $\mu = F_f/N \approx 0.02$ [29].
- 2) The gravitational acceleration is taken to be constant, yielding $g \approx 9.81 \text{ m/s}^2$ [30].
- 3) For a conventional flight, the mass of the aircraft is not constant (equal to MTOW) due to the fuel burn. However, constant mass is a valid assumption for a battery–electric aircraft during a similar flight.
- 4) The efficiency from battery to propulsion is taken to be constant throughout the flight, with a value of $\eta_{\text{tot}} = 0.78$ [18], where the propeller, gearbox, electric motor, and power electronics have assumed efficiencies of 80%, 98%, 95%, and 98%, respectively. The value of the total efficiency is the product of all the individual efficiencies that are given in (1) and Fig. 4. Due to componentwise losses (inefficiencies) in the system, the power and energy requirements increase upstream from

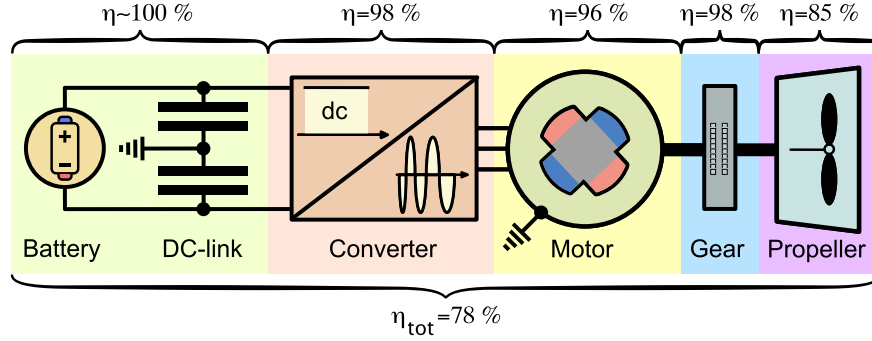


Fig. 4. Battery–electric propulsion system’s efficiencies by component [18].

the propeller. These components have lower losses under low currents at light load conditions

$$\eta_{\text{tot}} = \eta_{\text{pec}} \cdot \eta_{\text{mot}} \cdot \eta_{\text{gear}} \cdot \eta_{\text{prop}}. \quad (1)$$

C. Linearization of Mission Profiles From Actual Flights

Using data from Flightradar24 [26], linearized mission profiles showing velocity and altitude as a function of time have been made for the different distances. Fig. 5(a) depicts an example of these profiles that are based on flight information from actual flights made between November 1 and November 11, 2020, with the linearization shown in Fig. 5(b). The climb rate for these mission profiles was not artificially adjusted for potential energy savings since Norway’s topography often limits these actions.

D. Estimation of Battery Power From a Mission Profile

Based on the simplified flight profiles, it is possible to calculate the power required from the battery as a function of time. Systematically, five different phases of the flight should be considered, which are highlighted in Fig. 5(c): 1) acceleration on the ground (takeoff); 2) acceleration in the air (climb); 3) cruise; 4) deceleration in the air (descent); and 5) deceleration on the ground (landing). In addition, holding and diversion to an alternative airport, if needed, are shown in Fig. 5(d).

In all the calculations, the effect of wind (D_w) has been ignored for simplicity. Moreover, the effect of regenerative soaring (breaking) and the use of flaps during deceleration has been omitted. However, the deceleration on the ground is taken to be thrust-free with the regeneration of kinetic energy.

In this numerical modeling framework, as shown in Fig. 3, the calculations were performed in the MATLAB computational environment. The results give the force as a function of time, which can then be multiplied by the velocity to yield the power. Using the linearized flight profiles from Fig. 5(b), the plots presented in Fig. 6 are obtained. It can be seen that takeoff and climb is the most power-demanding part of the flight.

E. Accumulation of Energy

Integrating the power over time gives us the total energy requirement for the mission profile of the flight. This has been

done numerically by taking the power to be constant in shorter time steps of ≤ 1 s, which is the basis for the rectangle or midpoint rule of integration. A plot of accumulative energy is shown in Fig. 6(b).

F. Sizing of Battery Capacity for a Complete Flight

The modeling provides detailed insights into the sizing of the battery’s energy content. However, as a benchmark to support the validity of the modeling, a simplified way to estimate battery energy needed for a given range, based on the modified Breguet equation [18], is

$$E_{\text{bat}} \approx E_{T\infty} = \frac{1}{\eta_{\text{tot}}} \frac{m_{\text{tot}} g}{L/D} R \quad (2)$$

where the equation is made independent of the cruising speed and only the cruising range is considered. Hence, the power, the L/D ratio, and the speed are assumed constant. However, when considering the reserve cruising time needed to reach a diversion airport [see Fig. 5(d)], the needed energy reservoir becomes

$$E_{\text{bat}} \approx E_{T\infty} + E_{\text{res}} = \frac{1}{\eta_{\text{tot}}} \frac{m_{\text{tot}} g}{L/D} (R + v_{\text{cruise}} \Delta t_{\text{res}}). \quad (3)$$

As depicted in Fig. 5(c), there will be important changes during the different phases of the flight, which are not covered by simplified calculations. Therefore, a detailed sizing of the battery capacity can be achieved using the actual $P-t$ curve estimated from the mission profile, yielding

$$E_{\text{bat}} = \underbrace{\frac{1}{\eta_{\text{tot}}} \frac{m_{\text{tot}} g}{L/D} v_{\text{cruise}} \Delta t_{\text{res}}}_{E_{\text{res}}} + \underbrace{\max \left[\int_0^t \frac{P}{\eta_{\text{tot}}} dt \right]}_{E_{\text{peak}}} + \underbrace{E_{\text{aux}}}_{\approx 0}. \quad (4)$$

Equation (4) implies the total energy of the battery can be calculated from the drained energy plotted in Fig. 6(b), accounting for the cruise, acceleration (takeoff and climb), and deceleration (descend and land). For simplicity, it is assumed that the energy required for auxiliary functions is accounted for in the mass, so it is set to zero. When breaking down the drained energy needed from the battery, it can be separated according to the following equation:

$$E_{\text{peak}} = E_{T\infty} + E_{\text{acc}}. \quad (5)$$

E_{peak} is found as the maximum values of the accumulated $E-t$ curve of the flight considered, while E_{res} is based on the certification requirement (EASA CS-23 or CS-25).

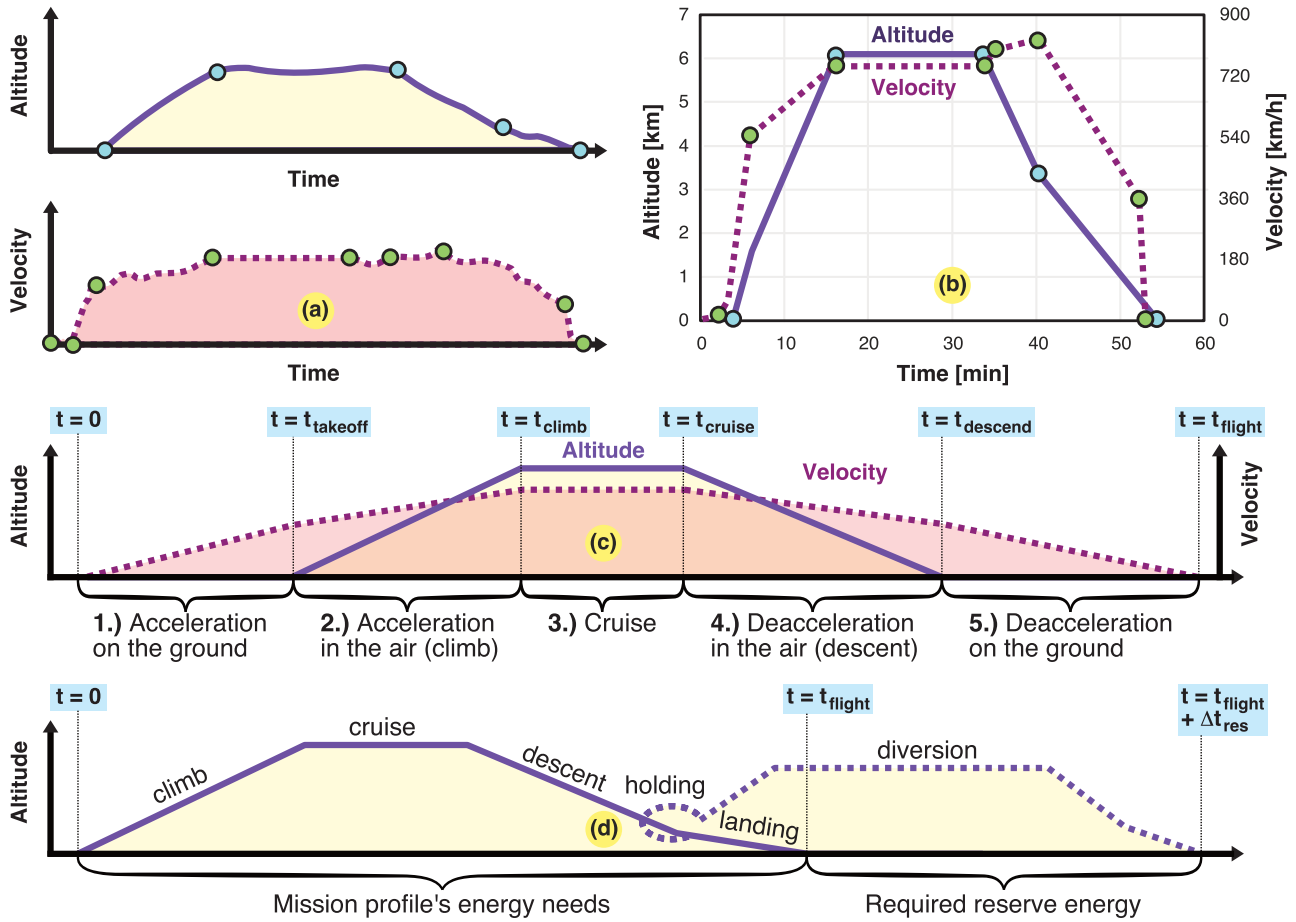


Fig. 5. (a) Illustration of actual altitude and velocity profiles collected from Flightradar24 [26]. (b) Circled points to depict the points transferred to the linearized mission profile. (c) Oversimplified mission profile with flight phases and key time instants indicated. (d) Full flight profile, including holding and diversion.

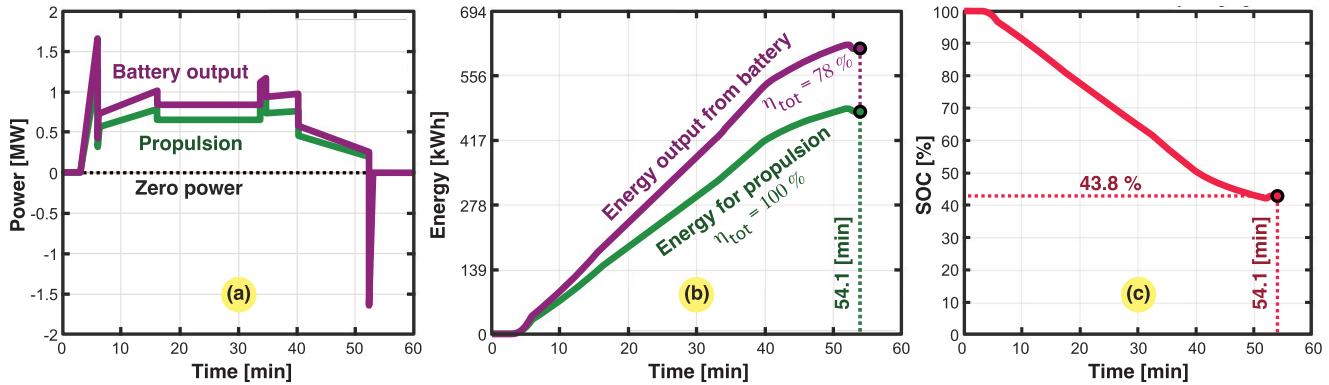


Fig. 6. Example for Case 1—Alice. (a) Power versus time for the linearized flight profile in Fig. 5(b) with the required power to deliver the specified thrust and the battery power required with $\eta = 78\%$. (b) Accumulative energy required to deliver the power in Fig. 6(a) for the flight profile in Fig. 5(b). Both the required energy for propulsion (or, equivalently, setting $\eta = 100\%$) and the required energy from the battery with 78% have been plotted. (c) Example of SOC for a battery during flight based on the accumulative energy consumption from Fig. 6(b) for the linearized flight profile in Fig. 5(b). It has been assumed that the battery is fully charged at the beginning of the flight.

Finally, when the energy needs have been established, the mass of the battery is estimated from

$$m_{\text{bat}} = \frac{E_{\text{bat}}}{e_{\text{bat}}}. \quad (6)$$

G. State-of-Charge Prediction

From the accumulative energy required from the battery, the state of charge (SOC) can be estimated [31], which

describes the immediate charge to maximum charge, where 100% implies a fully charged battery. Alternatively, the depth of discharge (DOD) is the amount of battery discharge, where 100% means fully discharged. To estimate the time-dependent SOC, an assumption on battery size must be made. For a given flight, the battery must be able to deliver at least as much energy as the peak of accumulated energy needed for the flight [i.e., the maximum value in Fig. 6(b)]. However,

TABLE IV
SUMMARY OF EQUATIONS APPLIED TO CALCULATE DELIVERED POWER AND TOTAL ENERGY CONSUMPTION

Phase of flight	Parameter	Equation
1. Acceleration on the ground (takeoff) / 5. Deacceleration on the ground (landing)	Force	$F = ma + D + F_f$
	Drag	$D = \frac{L}{L/D}$
	Lift	$L = mg \left(\frac{v}{v_{climb}} \right)^2$
	Friction	$F_f = \mu(mg - L)$
	Power	$P = Fv$ $P_{bat} = P/\eta_{tot}$
	Energy	$E = \int_0^{t_{takeoff}} P dt$ or $E = \int_{t_{descend}}^{t_{flight}} P dt$ $E_{bat} = E/\eta_{tot}$
2. Acceleration in the air (climb) / 4. Deacceleration in the air (descent)	Force	$F = ma + D + mg \sin(\theta)$
	Drag	$D = \frac{L}{L/D}$
	Lift	$L = mg \cos(\theta)$
	Power	$P = Fv$ $P_{bat} = P/\eta_{tot}$
	Energy	$E = \int_{t_{takeoff}}^{t_{climb}} P dt$ or $E = \int_{t_{cruise}}^{t_{descend}} P dt$ $E_{bat} = E/\eta_{tot}$
	3. Cruise at constant altitude and velocity	Force
Drag		$D = \frac{L}{L/D}$
Lift		$L = mg$
Power		$P = Fv$ $P_{bat} = P/\eta_{tot}$
Energy		$E = \int_{t_{climb}}^{t_{cruise}} P dt$ $E_{bat} = E/\eta_{tot}$

this does not necessarily imply that this is sufficient. Not only does one have to account for reserves but also the same plane might be used for different routes, meaning that the total energy of the battery may be much higher than the peak of accumulative energy for a specific flight. To limit the complexity of the calculations, it is assumed that the energy available onboard the aircraft is enough for that exact route.

The energy required for reserves is calculated as 1 h flight at cruise velocity (further explained in Appendix A in the Supplementary Material). The equations in Table IV are used to calculate reserves for cruising conditions, where the free-body diagram depicted in Fig. 7 is utilized. To find the energy required from the battery, this energy is then divided by the overall propulsion efficiency (η_{tot}). The SOC in the battery can be approximate according to (7) if the battery voltage is assumed independent of the SOC, where $SOC_{min} \approx (E_{bat} - E_{peak})/E_{bat}$

$$SOC(t) \approx \frac{E_{bat} - \int_0^t P_{bat} \cdot dt}{E_{bat}}. \quad (7)$$

H. Estimation of Battery Mass

To determine the mass of the battery pack, different values of specific energy have been considered.

- 1) Existing SotA battery technology has an energy density ~ 260 Wh/kg (i.e., Eviation's Alice), which has an overall energy storage mass fraction of 60%.
- 2) For comparison, the most common jet fuel has a specific energy of 11900 Wh/kg [18], without considering the tank, which still causes the fuel's overall weight fraction to be in the range 20%–40%.
- 3) Near-term future battery technology is projected to have 400–500 Wh/kg in energy density.
- 4) Possible 10–20 years' perspective, considering new technologies, such as Li-S or Li-air (~ 1000 Wh/kg).

The total energy required by the battery for the different distances is found using (4) and (5), where the electric power train's overall efficiency (η_{tot}) is included. The battery weight is calculated by dividing the battery energy by the energy density. Three values for the battery weight are obtained for

TABLE V

BATTERY MASS AND FRACTION OF AIRCRAFT MASS FOR THE FLIGHT PROFILE IN FIG. 6(B) FOR DIFFERENT BATTERY TECHNOLOGY SCENARIOS FOR BOTH CASE STUDIES FOR CASE 1 (ALICE) AND CORRESPONDINGLY FOR CASE 2 (DHC-100) USING (6)

Aircraft	E_{bat}	m_{tot}	Conservative		Moderate		Optimistic	
			$e_{bat} = 260 \text{ Wh/kg}$	$e_{bat} = 500 \text{ Wh/kg}$	$e_{bat} = 1000 \text{ Wh/kg}$	$e_{bat} = 260 \text{ Wh/kg}$	$e_{bat} = 500 \text{ Wh/kg}$	$e_{bat} = 1000 \text{ Wh/kg}$
			m_{bat}	m_{bat}/m_{tot}	m_{bat}	m_{bat}/m_{tot}	m_{bat}	m_{bat}/m_{tot}
Case 1	1074 kWh	6350 kg	4132 kg	65 %	2149 kg	34 %	1074 kg	17 %
Case 2	3659 kWh	15 966 kg	14 074 kg	88 %	7318 kg	46 %	3659 kg	23 %

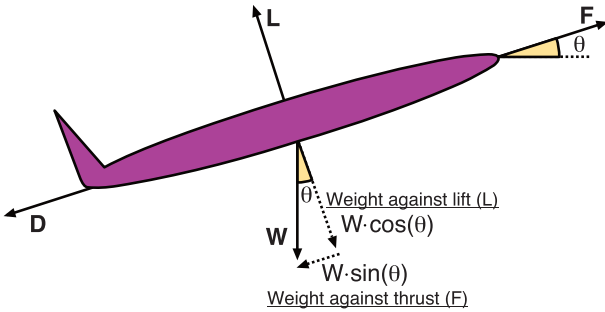


Fig. 7. Free-body diagram of the aircraft under climb where the weight is decomposed into components in the direction of the thrust and the lift, respectively.

each plane, depending on the technology level (see Table V as a preview result for Fig. 6).

I. Range Optimization

Maximizing electric aircraft range boils down to optimizing the following:

- 1) maximizing the specific energy of the battery (e_{bat});
- 2) maximizing the total efficiency of the propulsion system, from the energy source to the delivered thrust (η_{tot}), including the electric propulsion system;
- 3) maximizing the aircraft's lift-to-drag ratio (L/D);
- 4) minimizing the mass-fraction of the battery compared to the total aircraft's mass (m_{bat}/m_{tot});
- 5) minimizing the mass of the electric propulsion system, including power electronics converter, electric motor, and the thermal management system;
- 6) minimizing the total mass of the aircraft (m_{tot}) by lowering the aircraft's structural weight.

IV. RESULTS

To study the technological feasibility of implementing electric planes in Norway, a case study was conducted using two different aircraft and five handpicked flight distances (from 77 to 392 km). Their linearized mission profiles are depicted in Fig. 8.

For each of the five chosen distances, the power ($P-t$ curve), energy consumption ($E-t$ curve), and the SOC curve have been estimated for both aircraft. Afterward, the required battery mass and resulting battery to total aircraft mass ratio for each case are summarized. Finally, based on the results, a discussion on the technological feasibility of implementing electric aircraft in Norway is made. This is followed

by a discussion of other factors affecting the possibility of implementing electric aircraft in Norway in Section V.

As an overview of the case studies, Table VI provides the basic metrics for the five different routes that have been studied. It can be seen that the ideal flight time, assuming constant velocity, is significantly lower than the actual flight time, taking other flight phases into account.

In Sections IV-A–IV-E, the performance results of each route will be presented in detail. To make the simulations, the assumed battery capacity could be estimated from (2) or (3), both assuming constant speed, with or without energy reserve for cruising to the diversion airport. However, (4) has been utilized to compute the actual $E-t$ curve to estimate the needed battery capacity, including energy reserves. The difference is clearly shown in Tables VII and VIII for each aircraft. This means that, when sizing the battery, simplified assumptions tend to be incorrect when compared to detailed calculations of the actual mission profile, which emphasizes one of the contributions of this work. In addition, the peak energy consumption (E_{peak}) found from each $E-t$ curve is used to calculate the minimum SOC (SOC_{min}). Generally, the longer the route, the lower the SOC_{min} becomes. This emphasizes the poor utilization of the battery, which also illustrates the problem when using existing certification requirements for a new product with different technical characteristics and operating conditions.

A. Rørvik–Namsos (77 km)

The first distance chosen for this study was from Rørvik to Namsos—a total of 77 km. This distance is originally operated by a DHC-100 aircraft. First, a linearized flight profile is illustrated in Fig. 8(a). Then, the resulting calculated power and energy consumption for this flight profile are shown in Appendix B in the Supplementary Material (see Fig. 10), along with the estimated SOC of the battery throughout the flight. It can be clearly seen that the cruising power is $<40\%$ of the peak power. The flight experiences a battery discharge of $<15\%$.

B. Stavanger–Bergen (160 km)

The second distance chosen for this study was from Stavanger to Bergen, a total of 160 km. This flight is operated around 11 times daily, making it an attractive route for the implementation of electric aircraft. Because of the frequency of flights, different airlines, and aircraft operators, the flight profile chosen is that of a Boeing 737. The linearized mission profile for this flight is illustrated in Fig. 8(b). The resulting

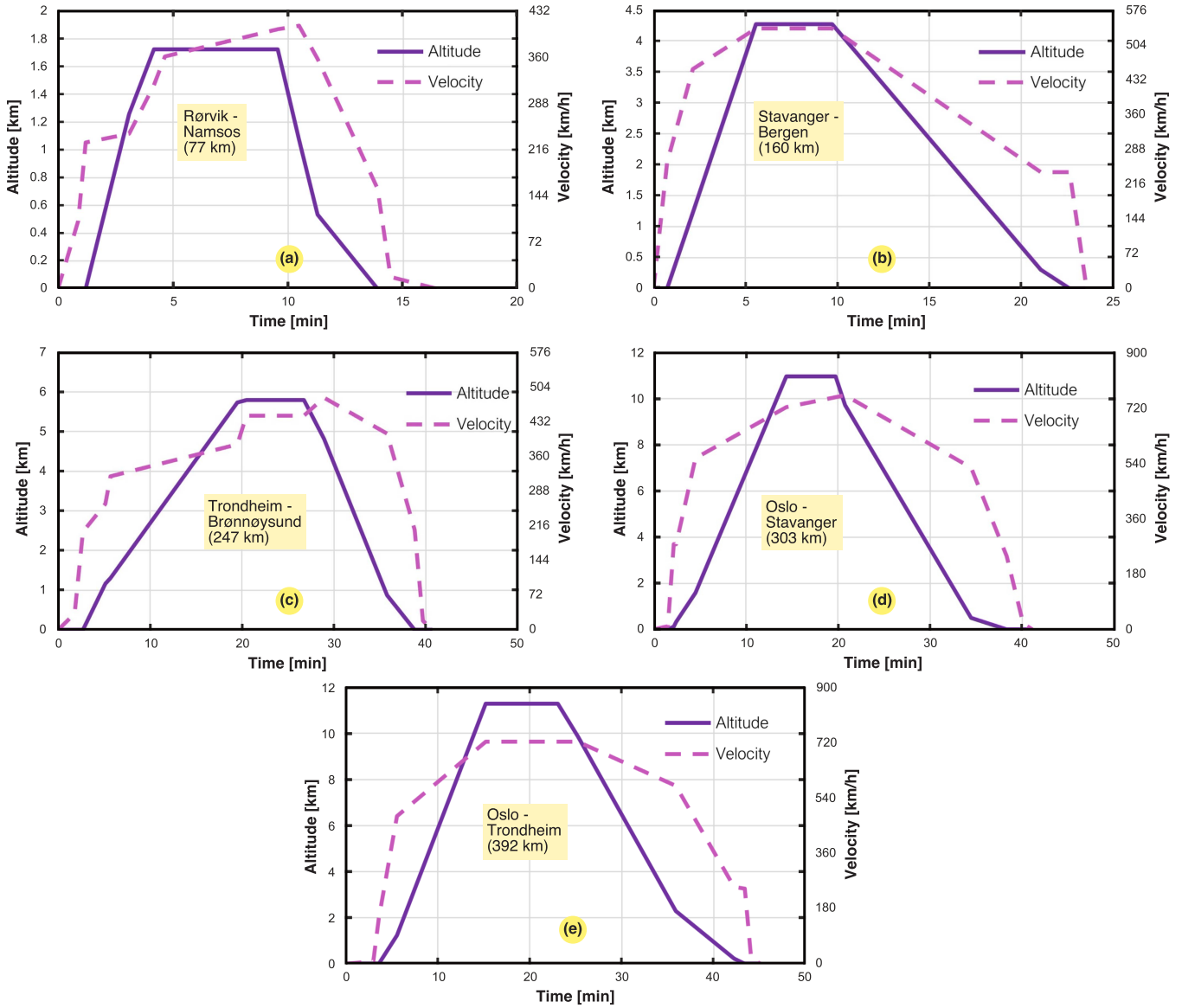


Fig. 8. Simplified mission profiles for five routes and estimated from three flights for each. (a) Rørvik–Namsos with a DHC-100 aircraft. (b) Stavanger–Bergen route based on three flights made by a Boeing 737 aircraft. (c) Trondheim–Brønnøysund with a DHC-100 aircraft. (d) Oslo–Stavanger with a Boeing 737 aircraft. (e) Oslo–Trondheim with a Boeing 737 aircraft.

TABLE VI
COMPARISON TRAVEL DISTANCE, CRUISING ALTITUDE, AND CRUISING SPEED OF EACH ROUTE, AND COMPARISON BETWEEN IDEAL FLIGHT TIME AND ACTUAL FLIGHT TIME FOR EACH MISSION PROFILE

Route	Travel distance (R)	Cruising altitude (h_{cruise})	Cruising speed (v_{cruise})	Flight time		
				Ideal (R/v_{cruise})	Actual (t_{flight})	Deviation
Rørvik-Namsos	77 km	1.7 km	386 km/h	12.0 min	16.5 min	+37.5 %
Stavanger-Bergen	160 km	4.3 km	539 km/h	17.8 min	23.5 min	+32.0 %
Trondheim-Brønnøysund	247 km	5.8 km	445 km/h	33.3 min	40.7 min	+22.2 %
Oslo-Stavanger	303 km	11.0 km	739 km/h	26.4 min	41.2 min	+56.1 %
Oslo-Trondheim	392 km	11.3 km	723 km/h	32.5 min	45.3 min	+39.4 %

calculated power and energy consumption for this flight profile are shown in Appendix B in the Supplementary Material

(see Fig. 11), along with the estimated SOC of the battery throughout the flight, with a final battery discharge of >25%.

TABLE VII

CASE 1: ALICE—SIZING COMPARISON OF BATTERY CAPACITY AGAINST ANALYTICS AND EVALUATION OF MINIMUM DISCHARGE

Route	Const. speed	Const. speed	Numerical sol.	$E - t$ curves	
	est. [18]	incl. 1 h res.	incl. 1 h res.	of Figs. 10-14	
	E_{bat} - eq. (2)	E_{bat} - eq. (3)	E_{bat} - eq. (4)	E_{peak}	SOC _{min}
Rørvik-Namsos	85.4 kWh	513.6 kWh	530.9 kWh	79.8 kWh	85.0 %
Stavanger-Bergen	177.5 kWh	775.3 kWh	628.4 kWh	174.6 kWh	72.2 %
Trondheim-Brønnøysund	274.0 kWh	767.6 kWh	711.1 kWh	259.9 kWh	63.5 %
Oslo-Stavanger	336.1 kWh	1155.8 kWh	869.4 kWh	419.2 kWh	51.8 %
Oslo-Trondheim	434.8 kWh	1236.8 kWh	891.0 kWh	436.2 kWh	51.0 %

TABLE VIII

CASE 2: DHC100—SIZING COMPARISON OF BATTERY CAPACITY AGAINST ANALYTICS AND EVALUATION OF MINIMUM DISCHARGE

Route	Const. speed	Const. speed	Numerical sol.	$E - t$ curves	
	est. [18]	incl. 1 h res.	incl. 1 h res.	of Figs. 10-14	
	E_{bat} - eq. (2)	E_{bat} - eq. (3)	E_{bat} - eq. (4)	E_{peak}	SOC _{min}
Rørvik-Namsos	286.3 kWh	1721.7 kWh	1845.2 kWh	266.0 kWh	85.6 %
Stavanger-Bergen	595.0 kWh	2599.3 kWh	2169.7 kWh	584.6 kWh	73.1 %
Trondheim-Brønnøysund	918.5 kWh	2573.5 kWh	2447.4 kWh	868.5 kWh	64.5 %
Oslo-Stavanger	1126.7 kWh	3874.8 kWh	2980.1 kWh	1402.0 kWh	53.0 %
Oslo-Trondheim	1457.7 kWh	4146.2 kWh	3049.5 kWh	1464.3 kWh	52.0 %

C. Trondheim–Brønnøysund (247 km)

The third distance, from Trondheim to Brønnøysund, is originally operated by a DHC-100 aircraft and is 247 km long. The linearized mission profile for this flight is illustrated in Fig. 8(c). The resulting calculated power and energy consumption for this flight profile are shown in Appendix B in the Supplementary Material (see Fig. 12), along with the estimated SOC of the battery throughout the flight. The flight has more power spikes distributed over the flight, but the cruising power is $>60\%$ of the peak power. As the range is longer than the second distance, the overall battery discharge is now higher and $>35\%$.

D. Oslo–Stavanger (303 km)

The fourth distance, from Oslo to Stavanger, is one of Norway's most frequent flight distances due to daily business travels (14th place in Europe overall [23]). The 303-km-long route had over 7000 flights in 2019 each way [19]. The linearized mission profile for this flight is illustrated in Fig. 8(d). The resulting calculated power and energy consumption for this flight profile are shown in Appendix B in the Supplementary Material (see Fig. 13), along with the estimated SOC of the battery throughout the flight (reaches nearly 50%). It has a similar power spike in magnitude for both takeoff and climbing, which is about 70% higher than the cruising power.

E. Oslo–Trondheim (392 km)

Finally, the fifth distance, from Oslo to Trondheim, is 392 km long and was the most flown domestic route in Norway in 2019 [19] (fifth place in Europe overall [23]). The linearized mission profile for this flight is illustrated in Fig. 8(e). The

resulting calculated power and energy consumption for this flight profile are shown in Appendix B in the Supplementary Material (see Fig. 14), along with the estimated SOC of the battery throughout the flight. The final charge of the battery is about 50% of its capacity, which is the highest utilization of all of the cases. Still, there is about 30% capacity left before entering into the deep discharge region of the battery.

F. Battery Mass and Mass Ratio

The calculation of the battery mass was achieved based on (4) and (6), which means that it includes 1 h of flight at cruise velocity as reserves. The total mass of the aircraft has been assumed constant, which means that an increase in battery mass only means an increase in the ratio and not in the total mass. The results for the different cases are presented in Table IX and graphically in Fig. 9.

V. DISCUSSION

A. Battery Mass Fractions and Limitations

In this work, the aircraft mass is assumed constant, and the mass fraction of batteries to total mass is used as a criterion of viability. The actual fuel accounted for in the MTOW of Dash 8-100 has a mass fraction ranging from 16% to 29% of the maximum takeoff weight, depending on whether the optional auxiliary tanks are used or not. This means that retrofitting a Dash 8-100 aircraft with batteries and electric engines would most likely be possible if the mass fraction of the batteries were $\leq 29\%$, considering the fact that the aircraft is already built to carry this weight in terms of fuel. However, more complex modifications would likely be required to reduce the aircraft's weight with higher mass fractions.

TABLE IX

BATTERY MASS AND FRACTION OF AIRCRAFT MASS FOR THE DIFFERENT DISTANCES IN THE CASE STUDY USING DIFFERENT BATTERY TECHNOLOGY LEVELS AND AIRCRAFT, BASED ON (6), WHERE CASE 1 IS ALICE AND CASE 2 IS DASH 8-100

Flight	Aircraft	Conservative		Moderate		Optimistic	
		$e_{bat} = 260 \text{ Wh/kg}$		$e_{bat} = 500 \text{ Wh/kg}$		$e_{bat} = 1000 \text{ Wh/kg}$	
		m_{bat}	m_{bat}/m_{tot}	m_{bat}	m_{bat}/m_{tot}	m_{bat}	m_{bat}/m_{tot}
Rørvik-Namsos (77 km)	Case 1	2042 kg	32 %	1062 kg	17 %	531 kg	8 %
	Case 2	7097 kg	44 %	3691 kg	23 %	1845 kg	12 %
Stavanger-Bergen (160 km)	Case 1	2417 kg	38 %	1257 kg	20 %	628 kg	10 %
	Case 2	8345 kg	52 %	4339 kg	27 %	2170 kg	14 %
Trondheim-Brønnøysund (247 km)	Case 1	2735 kg	43 %	1422 kg	22 %	711 kg	11 %
	Case 2	9413 kg	59 %	4895 kg	31 %	2447 kg	15 %
Oslo-Stavanger (303 km)	Case 1	3344 kg	53 %	1739 kg	27 %	870 kg	14 %
	Case 2	11 462 kg	72 %	5960 kg	37 %	2980 kg	19 %
Oslo-Trondheim (392 km)	Case 1	3427 kg	54 %	1782 kg	28 %	891 kg	14 %
	Case 2	11 729 kg	73 %	6099 kg	38 %	3050 kg	19 %

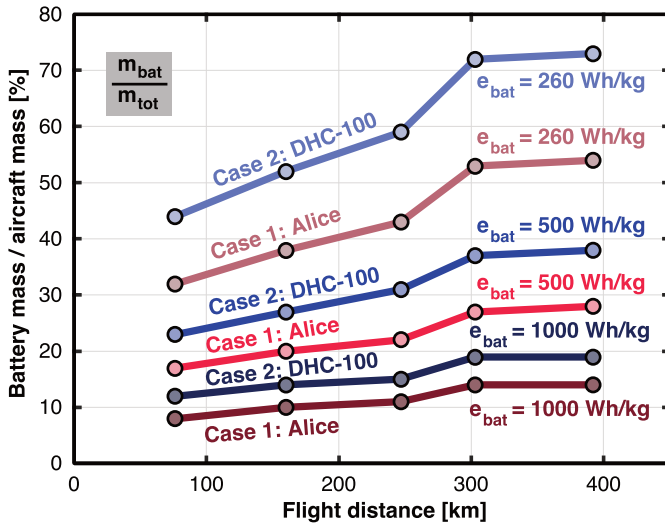


Fig. 9. Battery mass ratio for the Alice and DHC-100 aircraft, as found for the different flight distances modeled in this case study (i.e., Figs. 10–14 in the Supplementary Material), depending on the battery technology level, projected based on (6).

The aircraft Alice represents the possibilities of an electric aircraft that is built from scratch, utilizing the advantages given by electric engines, such as tip-mounted propellers and distributed propulsion. The battery’s mass to total aircraft mass fraction achieved in Alice is 60% [24]. Scaling up an aircraft usually allows for higher L/D ratios and higher fuel to MTOW ratios; however, it is difficult to say how Alice scales due to the highly unique design. Therefore, 60% has been maintained as a maximum achievable battery to total aircraft mass ratio if the aircraft is built from scratch as an electric aircraft with a novel design for up to 19 passengers.

To achieve a mass fraction of batteries under 40% with a retrofitted Dash 8-100 aircraft, improved battery technology compared to the current SotA is required. With current technologies, the shortest flight from Rørvik to Namsos (77 km) requires a battery mass fraction of 44%, while the longest requires a battery mass fraction of 73%. If batteries can reach

a much-claimed energy density of 500 Wh/kg, all the flight distances in this study would require a mass fraction of the batteries under 40%. The Alice aircraft, on the other hand, can carry out all the missions with a battery mass fraction ranging from 32% to 54% (see Table IX). This was expected, as Eviation claims the aircraft has a range of 440 nautical miles (815 km), with its actual battery mass fraction being 60%. A 19-passenger aircraft designed to be electric (a “scaled-up” version of the Alice aircraft) using SotA batteries ($e_{bat} = 260 \text{ Wh/kg}$) would likely be somewhere between the plot of the Alice aircraft and the Dash 8-100 aircraft in Fig. 9. If a battery mass fraction of roughly 60% were achievable, the range of such an aircraft using the profiles estimated in this study would be around 300 km, including reserves. All but the longest flight distances considered in this study would be possible with a range of 303 km. More details on the commercial batteries available and the future projections are given in Appendix C in the Supplementary Material. Table X gives a summary of the challenges discussed for the implementation of electric flight.

B. Key Solutions to Battery–Electric Challenges

Considering the abovementioned observations in terms of mass, there are two clear paths that can enable deep electrification of the aircraft fleet and operate all the domestic flight distances in Norway:

- 1) improved gravimetric energy density of battery technology [15];
- 2) novel aircraft design from scratch with lower structural weight, higher aerodynamic efficiency, and use of multifunctional materials [32], [33], [34].

The first option gives the best alternative in terms of investment cost and simplicity, while the second is independent of the developments and breakthroughs in the battery industry. Like the range, the mass fraction is influenced by the aerodynamic efficiency (L/D), the power train efficiency (η_{tot}), and the specific gravimetric energy of the battery (e_{bat}). Improving any one of these factors would, therefore, augment

the chances of achieving a low enough battery mass fraction for a given distance so that the aircraft in question could be operated electrically.

C. Limitations in Power Train Efficiency

The power train efficiency (η_{tot}) has been assumed to be constant, with a value of 78%. However, Wang *et al.* [35] showed that, for a particular setup, the efficiency varies from 92% to 95% for the motor and 92.5% to 93.5% for the power electronics controller with rotational speeds ranging from 1300 to 2600 rpm. Still, these efficiencies would be enhanced as the power level is scaled up. However, for the propeller, the efficiency varies from roughly 50% to 80% in the same interval [35]. Moreover, Ma *et al.* [36] obtained similar results, showing controller efficiencies in the range of 91.5%–94.2%, motor efficiencies between 92.5% and 93.5%, and propeller efficiencies between 67% and 83% with rotational speeds varying from 1300 to 2200 rpm. Therefore, propellers must be optimized for a certain operating range, which results in lower efficiency in other parts of the flight. It also shows that assuming constant efficiency with a value of 78% is quite optimistic. In the worst case for a small ground test aircraft, using the values from the study made by Wang *et al.* [35] and including the gearbox would give us a total efficiency of 63.4%–64.5%. More details and specifics regarding realistic energy efficiencies for SotA components are provided in Appendix D in the Supplementary Material.

D. Peak Power Propulsion Requirement

If the power train for an electric motor is considered, one can see that the efficiency from the motor to propulsion is not the same as the efficiency from the battery to propulsion. However, because the difference is only 2%, the battery power requirement has been used to discuss the motor power requirement. The largest existing motor is the Magni500 by MagniX, delivering continuous power of 560 kW. Bigger motors, such as Siemens's SP2000D and the 2-MW motor from MagniX, are still in the testing and verification phase. For the DHC-100 aircraft, the peak power requirements for the different distances are approximately 3.3, 4, 2.3, 4, and 3.8 MW ordered from the shortest to the longest distance. However, this is mainly in the takeoff and climbing phases and would mean that the motors required for peak power would be unnecessarily oversized for the rest of the flight. The fact that such high power is required for a short period of time is an issue that has been discussed in the literature [37]. The electric motor has the advantage that it maintains relatively high efficiency over a large window of rotational speeds [35].

Therefore, for the Dash 8-100 retrofitted electric aircraft, as many as seven to eight motors would be required with SotA technology to deliver the required power for takeoff given by the flight profiles applied in this study. However, for the Alice aircraft, the peak power requirement is much lower, giving values of 1.2, 1.4, 0.8, 1.5, and 1.4 MW for the flight distances from shortest to longest. It is relevant to note that the actual installed power in Alice is only 900-kW peak power and 260 kW at cruise [24]. This means

that the given profiles are not achievable with the Alice aircraft. This indicates that the profiles for altitude and velocity applied here are not optimized for use with an electric aircraft.

The peak power requirement for the distance Trondheim–Brønnøysund is not during takeoff but rather during acceleration right before reaching cruising conditions. Comparing the power requirement calculated for the Dash 8-100 aircraft in the two cases, one can note that the shortest distance (Rørvik–Namsos) has a peak power of 3.3 MW during takeoff, while the longer distance (Trondheim–Brønnøysund) has a peak power of 1.8 MW during takeoff due to a lower acceleration, which requires a longer takeoff length. Therefore, a tradeoff exists between short takeoff length and reduced peak power. Reducing installed motor capacity would reduce the weight of the aircraft, which would reduce the general energy requirement but would give a longer takeoff length.

E. Additional Battery Power Density Requirement

The highest peak power required from the battery has been calculated to be ~ 4 MW for the Dash 8-100 aircraft for the distances Stavanger–Bergen, Oslo–Stavanger, and Oslo–Trondheim. The battery used in Eviation's Alice weighs 3600 kg and must be capable of delivering a claimed peak power of 900 kW, which amounts to a power density of 0.25 kW/kg. Considering a power density in the range of 0.25–0.5 kW/kg, an 8000–16 000-kg battery would be required to deliver 4-MW peak power to the Dash 8-100 aircraft. This amounts to a battery mass fraction of 50%–100% if the mission profile stays unchanged. However, using SotA batteries, the energy required for these same flights also puts the battery mass fraction between 52% and 73%. It becomes clear that increasing the energy density of the batteries without also achieving a higher power density would not help in reducing the battery mass fraction on board the aircraft. This could be a challenge, as increased energy density often means reduced power density. To achieve batteries suited for aviation, efforts should be made to find batteries that are not only energy-dense but also have high specific power density. Even though the power density of Eviation's Alice is limiting, the power density of batteries does not necessarily need to be as low as 250 W/kg. Modern Li-ion batteries can reach a power density as high as 1200 W/kg [38], while electric vehicle grade batteries already reach 650 W/kg [39].

One investigated solution to the problem of power density is the use of supercapacitors. The power density of supercapacitors is on the order of 10 kW/kg [37], which means that 400 kg of supercapacitors could deliver the necessary peak power of 4 MW. The problem is that the energy density is low, currently on the order of 10 Wh/kg for commercialized systems [37]. Ongoing research is working to improve the energy density of supercapacitors, and laboratory-stage experiments have shown energy densities from 50 to 150 Wh/kg [37]. Alone, supercapacitors do not deliver sufficient energy for flight, but a functioning solution could still be using a combination of supercapacitors for takeoff and climb, and batteries for the rest of the flight, or hybrid supercapacitors [40].

F. Safety Considerations

One safety issue that has already been addressed in the calculations is the required energy reserves. The reserves are necessary in case of unforeseen events but also add a large amount of weight to achieve the required battery capacity. This is especially limiting for first-generation electric aircraft, which would likely be operated over many distances that are shorter than 1-h total flight time.

Another major concern is the thermal runaway in batteries, a cascading, self-feeding exothermic reaction that can cause battery fires [41], [42]. Thermal runaway can be triggered by mechanical abuse (e.g., crushing or penetration), chemical abuse (e.g., overcharging or short-circuiting), or thermal abuse (e.g., excessive external temperatures) [41], [42]. Ongoing research is trying to understand the mechanisms behind thermal runaway in order to propose suited solutions [43]. Feng *et al.* [44] discussed some of the thermal runaway mechanisms and proposed a protection concept for thermal runaway. In addition to the thermal runaway issues, elevated temperatures accelerate the formation of a passivating solid electrolyte interphase (SEI) layer on the electrode surface [41], [42]. The formation of SEI is one of the main aging mechanisms of a lithium-ion battery (LIB), so faster SEI growth would result in more frequent replacement of the battery and higher maintenance costs. In addition to this, the performance of an LIB is very dependent on the temperature, and it is important to maintain it in its operating range [45].

Extensive testing and verification will be required for a novel aircraft concept, which increases the time that it would take to bring an electric aircraft to the market. Retrofitting a traditional aircraft with batteries and electric motors would likely reduce the time to market compared to a completely novel aircraft design because fewer tests would be required. As has been illustrated, retrofitting a modern aircraft with today's batteries does not give sufficient range without making some modifications to the structure. Such modifications would require further testing and verification, which would again increase the time to market. Therefore, until the batteries perform better, an extensive process of testing and verification should be expected with any electric aviation concept.

G. Critical Discussion on the Model Sensitivity

An effort has been made to illustrate the important influence of acceleration and climb on the energy and power demand, especially during short flights. Even though the modeling is more detailed-level than electric aircraft feasibility studies in the past, the model also has several weaknesses that should be addressed.

First and foremost, it is important to point out that many simplifications have been made, such as ignoring the effects of wind, assuming constant properties (such as L/D and g), and estimating unknown quantities (such as the L/D ratios and the takeoff velocity). Therefore, the calculated power and energy plots are to be seen as estimates. Also, the results indicate that the assumed properties have sensitivity to accuracy. The Alice aircraft has a peak power of 900 kW, while the calculated peak powers' range for actual mission profiles is not optimized for an electric flight ranges from 800 to 1500 kW. One solution could be that the velocity of liftoff from the ground was

assumed too high or the L/D ratio is higher than the value assumed. However, the most likely explanation is that the acceleration for the applied profiles is much higher than the design acceleration of the Alice aircraft during takeoff. More details on the physical model are provided in Appendix A in the Supplementary Material.

A second assumption that was made with respect to the collected data from Flightradar24 was that the velocity is given in the aircraft's direction of flight [26], not in the horizontal direction. If this assumption turns out to be wrong, the actual flight velocity would be lower than what has been assumed, and lower values of power and energy would be obtained.

Another major inaccuracy is that the model is based on a few data points, not only to make the simplified profiles but also on the actual profiles found on Flightradar24. The exact point of liftoff from the ground was not specified in the models on Flightradar24 and had to be estimated. Also, acceleration could only be found between actual data points, which has likely led to some inaccuracies. A low sampling rate can give inaccurate data, which then causes errors in calculated power requirements.

The power calculated is also based on sections of constant acceleration. Therefore, the transitions are quite abrupt compared to what they would be in a real flight. The plane does not suddenly jump from one acceleration and flight angle to another. Also, the flight profiles showed quite big variations for the same flight carried out at different times. This can be due to the operational freedom of the pilots or variations in operating conditions, such as turbulence or wind.

The fact that the flight profiles are taken from actual flights is both a strength and a weakness of this model. On the one hand, it gives a more accurate representation of what a flight would look like in terms of power and energy requirements. On the other hand, the aircraft operating the actual flights have different optimal flying conditions than the aircraft used in the model. In fact, three of the flights are operated by a Boeing 737. This aircraft has a higher cruise velocity and operating altitude than, for example, Widerøe's DHC-100 aircraft, and higher than what a first-generation electric aircraft would have. In fact, the Alice aircraft has an operational ceiling of 12 500 ft (3.81 km) and a cruise velocity of 220 knots (407 km/h) [24]. Therefore, it would be incapable of operating at the conditions determined by the Boeing 737, reaching over 10 000 m for the flights from Oslo to Stavanger and Oslo to Trondheim. All but the first flight in this study is operated at altitudes above 3.81 km and velocities above 407 km/h.

The lack of available data for the Alice aircraft makes this challenging. Therefore, sizing effects have not been considered. As argued by Pernet *et al.* [46], retrofitting an aircraft without resizing it for the given range makes the results look pessimistic compared to what would actually be achievable if the design is adapted to the operation range. In fact, it is observed that the peak power on the flights originally operated by DHC-100 aircraft is lower than the peak power of flights originally operated by a Boeing 737.

Another assumption made was that the battery capacity is adapted to the specific flight operated. The same plane operates

TABLE X
SUMMARY OF CHALLENGES FOR ELECTRIC AVIATION

Eviation Alice		De Havilland Canada Dash 8-100 (DHC-100)	
Limitations	Possible solutions	Limitations	Possible solutions
Battery mass The battery mass must be kept below 60 % of the total aircraft weight.	The current design with a battery capacity of 260 Wh/kg has been shown to yield a range of 303 km. Further increases in battery capacity would extend this range without changing the mass of the battery.	Development of batteries with 500 Wh/kg energy capacity would maintain the battery mass below 40 % in all routes presented in this study.	The battery mass must be kept below 40 % of the total aircrafts weight.
Powertrain efficiency Although there is variation in power-train component efficiency, the largest variation is in the propeller efficiency. In addition, the efficiency is lower than the electric components.	Propellers must be optimized to the specific operating range of the electric motor used to enhance efficiency.	Same as for Eviation Alice.	Same as for Eviation Alice.
Peak power The peak power requirement for the initial stages of taking off and climbing are up to 1.5 MW.	Considering current SotA technology, up to 3 electric motors would be required to achieve this peak power.	The peak power requirement for the initial stages of taking off and climbing are up to 4 MW. Considering current SotA technology, up to 8 electric motors would be required to achieve this peak power.	Peak power can be alleviated with longer take-off lengths, or higher power electric motors. Longer take-off lengths may require alterations to existing runways, whereas larger electric motors may compromise aircraft mass.
Battery power density The power density of the aircraft is 260 kW/kg when considering the total aircraft weight. This results in a battery that is 60 % of the weight of the aircraft.	Although the current system is sufficient, modern Li-ion batteries with higher power densities can ensure this is not a limitation.	Modern Li-ion batteries with higher power densities will help overcome this limitation, but super capacitors or hybrid super capacitors should be considered to increase the short-term power density requirements.	If the power density of the aircraft is 250 kW/kg when considering the total aircraft weight, the battery would have a mass fraction close to 100 % of the total aircraft weight.

several different routes during the day. Nonetheless, if the battery has exactly enough energy to operate the route in question, it gives a way of deciding whether the aircraft would be able to operate that route and shorter routes. This assumption only gives inaccurate curves for SOC because the total capacity of the battery would be higher than the one assumed if the aircraft also operated longer distances.

H. Future Research Items

This article's power and energy requirements are estimates due to the lack of high-resolution flight data and the assumptions made on the parameters. A more detailed study of a chosen flight distance, where more data points are included, and several graphs are plotted for the same distance, would give a better picture of both power and energy requirements and variations of these over the same operating distance. Moreover, the maximum takeoff length for a given airport should be included as a parameter to determine the minimum peak power requirement. A further study on the effect of varying parameters, such as the L/D ratio and the overall efficiency of the power and energy demand, should also be included for a complete analysis.

A more detailed plot of the power required from the battery versus time would also be a useful tool for testing how a battery discharged at these conditions would perform. Moreover, further work should study the effects on the battery performance and aging of operating different flights throughout the day, with varying charge and discharge profiles.

To further investigate the possibility of a 19-passenger electric aircraft with SotA batteries, a scaling analysis should be performed on the Alice aircraft to determine how parameters, such as the L/D ratio, the battery mass fraction, and the weight scale with increasing capacity.

Combining supercapacitors with batteries (or hybrid supercapacitors) in operating the electric motor could be investigated to reduce the total required battery mass in the aircraft and reduce the maximum discharge load. However, if sufficient takeoff lengths are allowed, the power density of the battery does not seem to be the main concern. Further studies on the battery performance while used in an aircraft would be needed to make conclusive remarks regarding this.

To be able to scale up battery-powered all-electric aviation in the future, the cost will be a major issue both in its construction and operation. These issues need to be studied as the technology matures further.

VI. CONCLUSION

In this article, light has been shed on the possibilities and limitations of implementing electric aircraft on domestic flights in Norway. Estimates on the power requirement, energy storage needs, and battery SOC were made for different distances. The results show that the battery mass fraction on a traditional 39-passenger aircraft retrofitted with electric engines and batteries would exceed the estimated maximum of 40% even for the shortest distance. Therefore, batteries with higher energy density are needed to retrofit existing aircraft without making large structural changes. However, other alternatives, such as novel aircraft designs, are a viable

option for implementing electric aircraft for distances up to 400 km with modern-day batteries. This is because aircraft designs from scratch allow for higher battery mass fractions due to lower structural weight and higher L/D ratios.

The nine-passenger electric aircraft used in this study showed battery mass fractions in the range of 32%–54% with SotA battery technology on distances from 77 to 392 km. It is worth noting that this is lower than the actual battery mass fraction of the actual aircraft under study (i.e., 60%), which shows that it would indeed be capable of providing sufficient energy for propulsion under all of the flights that were considered.

The peak propulsion power required to operate the aircraft over different distances was found during the takeoff phase of the flight, and it depends highly on the acceleration characteristics of the mission profile. It is generally seen that a faster acceleration phase shortens the takeoff length, but it significantly increases the aircraft's peak power requirement. Using the 39-passenger retrofitted aircraft, a power requirement of roughly 4 MW was found during takeoff for the fastest acceleration profile, while the slowest acceleration gave a power requirement of roughly 1.8 MW. For the nine-passenger electric aircraft, the power needed during takeoff was significantly lower, ranging from roughly 0.65 to 1.4 MW. This aircraft has 900-kW installed peak power, which means that only the acceleration giving 0.65 MW would be acceptable. Therefore, the takeoff length is an important parameter that would decide the maximum required power and, thereby, the number of installed motors.

This work finds that the SotA batteries are not sufficiently energy-dense to operate any of the given distances with an acceptable mass fraction in a retrofitted aircraft. The power density, on the other hand, may be sufficient if a longer takeoff distance can be allowed. Moreover, with innovative designs giving room for a higher mass fraction of batteries, energy densities may be sufficient, and power densities are also within acceptable limits. Based on these observations, two technological paths exist for making regional-electric flights a reality:

- 1) Improving existing battery technology, especially in terms of specific energy density. Moreover, the use of hybrid supercapacitors to deliver high power capacity and peak-shaving opportunities could reduce the overall weight and soften the power requirement from the battery.
- 2) Building a novel electric aircraft from scratch with properties of lower structural weight that allow a higher battery mass fraction. This would imply weight reduction of the aircraft, but another metric would be enhancing its L/D ratio to improve the aircraft's aerodynamic efficiency.

Finally, even though these results lay the groundwork for further opportunities within regional-electric flights, a lot of additional issues remain to be studied to make it take off. However, with the rapid development of electrochemical energy storage, such electrification may ascend rapidly soon, even faster than first envisaged.

REFERENCES

- [1] European Union. *Climate Action: Reducing Emissions from Aviation*. Accessed: Feb. 25, 2022. [Online]. Available: https://ec.europa.eu/clima/eu-action/transport-emissions/reducing-emissions-aviation_en
- [2] EUROCONTROL. (2021). *Data Snapshot #2 on CO₂ Emissions from Flights in 2020*. [Online]. Available: <https://www.eurocontrol.int/publication/eurocontrol-data-snapshot-co2-emissions-flights-2020>
- [3] Statista. *Annual Growth in Global Air Traffic Passenger Demand from 2006 to 2021*. Accessed: Feb. 25, 2022. [Online]. Available: <https://www.statista.com/statistics/193533/growth-of-global-air-traffic-passenger-demand/>
- [4] B. H. H. Goh *et al.*, "Recent advancements in catalytic conversion pathways for synthetic jet fuel produced from bioresources," *Energy Convers. Manag.*, vol. 251, Jan. 2022, Art. no. 114974.
- [5] C. A. Horowitz, "Paris agreement," *Int. Legal Mater.*, vol. 55, no. 4, pp. 740–755, 2016.
- [6] Rolls-Royce. (2021). *Rolls-Royce and Tecnam Join Forces With Widerøe to Deliver an All-Electric Passenger Aircraft Ready for Service in 2026*. [Online]. Available: <https://www.rolls-royce.com/media/press-releases/2021/11-03-2021-rr-and-tecnam-join-forces.aspx>
- [7] B. Sarlioglu and C. T. Morris, "More electric aircraft: Review, challenges, and opportunities for commercial transport aircraft," *IEEE Trans. Transport. Electric.*, vol. 1, no. 1, pp. 54–64, Jun. 2015.
- [8] J. K. Nøland, M. Leandro, and J. A. Suul, "High-power machines and starter-generator topologies for more electric aircraft: A technology outlook," *IEEE Access*, vol. 8, pp. 130104–130123, 2020.
- [9] D. Golovanov *et al.*, "4-MW class high-power-density generator for future hybrid-electric aircraft," *IEEE Trans. Transport. Electric.*, vol. 7, no. 4, pp. 2952–2964, Dec. 2021.
- [10] E. Sayed *et al.*, "Review of electric machines in more-/hybrid-/turbo-electric aircraft," *IEEE Trans. Transport. Electric.*, vol. 7, no. 4, pp. 2976–3005, Dec. 2021.
- [11] S. Li, C. Gu, M. Xu, J. Li, P. Zhao, and S. Cheng, "Optimal power system design and energy management for more electric aircrafts," *J. Power Sources*, vol. 512, Nov. 2021, Art. no. 230473.
- [12] S. Li, C. Gu, P. Zhao, and S. Cheng, "A novel hybrid propulsion system configuration and power distribution strategy for light electric aircraft," *Energy Convers. Manag.*, vol. 238, Jun. 2021, Art. no. 114171.
- [13] T. C. Cano *et al.*, "Future of electrical aircraft energy power systems: An architecture review," *IEEE Trans. Transport. Electric.*, vol. 7, no. 3, pp. 1915–1929, Sep. 2021.
- [14] A. Barzkar and M. Ghassemi, "Electric power systems in more and all electric aircraft: A review," *IEEE Access*, vol. 8, pp. 169314–169332, 2020.
- [15] A. W. Schäfer *et al.*, "Technological, economic and environmental prospects of all-electric aircraft," *Nature Energy*, vol. 4, no. 2, pp. 160–166, Feb. 2019.
- [16] P. J. Ansell and K. S. Haran, "Electrified airplanes: A path to zero-emission air travel," *IEEE Electr. Mag.*, vol. 8, no. 2, pp. 18–26, Jun. 2020.
- [17] S. Sripad and V. Viswanathan, "The promise of energy-efficient battery-powered urban aircraft," *Proc. Nat. Acad. Sci. USA*, vol. 118, no. 45, Nov. 2021.
- [18] M. Hepperle. (2012). *Electric Flight-Potential and Limitations*. [Online]. Available: <https://elib.dlr.de/78726/1/MP-AVT-209-09.pdf>
- [19] SSB. *Air Transport (Norwegian Data)*. Accessed: Feb. 25, 2022. [Online]. Available: <https://www.ssb.no/en/transport-og-reiseliv/luftfart/statistikk/lufttransport>
- [20] SSB. *Electricity (Norwegian Data)*. Accessed: Feb. 25, 2022. [Online]. Available: <https://www.ssb.no/en/energi-og-industri/energi/statistikk/elektrisit>
- [21] L. A.-W. Ellingsen, B. Singh, and A. H. Strømman, "The size and range effect: Lifecycle greenhouse gas emissions of electric vehicles," *Environ. Res. Lett.*, vol. 11, no. 5, May 2016, Art. no. 054010.
- [22] V. Viswanathan and B. M. Knapp, "Potential for electric aircraft," *Nature Sustainability*, vol. 2, no. 2, pp. 88–89, Feb. 2019.
- [23] Telegraph. (2017). *Europe's Busiest Air Routes? They Might Surprise You*. [Online]. Available: <https://www.telegraph.co.uk/travel/destinations/europe/articles/europe-busiest-air-routes/>
- [24] Eviation. *Alice*. Accessed: Feb. 25, 2022. [Online]. Available: <https://www.eviation.co>
- [25] Widerøe. *Aircraft Fleet*. Accessed: Feb. 25, 2022. [Online]. Available: <https://www.wideroe.no/en/about-wideroe/fleet>
- [26] Flightradar24. *Live Air Traffic Data*. Accessed: Feb. 25, 2022. [Online]. Available: <https://www.flightradar24.com>
- [27] P. M. Sforza, "Direct calculation of zero-lift drag coefficients and (L/D)_{max} in subsonic cruise," *J. Aircr.*, vol. 57, no. 6, pp. 1224–1228, Nov. 2020.
- [28] F. I. Romli and M. S. Kamaruddin, "Preliminary study of emissions regulation effects on future commercial aircraft designs," *Int. J. Environ. Sci. Develop.*, vol. 4, no. 2, p. 187, 2013.
- [29] Engineering-ToolBox. *Rolling Resistance*. Accessed: Feb. 25, 2022. [Online]. Available: https://www.engineeringtoolbox.com/rolling-friction-resistance-d_1303.html
- [30] Engineering-ToolBox. *U.S. Standard Atmosphere*. Accessed: Feb. 25, 2022. [Online]. Available: https://www.engineeringtoolbox.com/standard-atmosphere-d_604.html
- [31] I. B. Espedal, A. Jinasena, O. S. Burheim, and J. J. Lamb, "Current trends for state-of-charge (SoC) estimation in lithium-ion battery electric vehicles," *Energies*, vol. 14, no. 11, p. 3284, Jun. 2021.
- [32] C. E. Jones *et al.*, "Electrical and thermal effects of fault currents in aircraft electrical power systems with composite aerostructures," *IEEE Trans. Transport. Electric.*, vol. 4, no. 3, pp. 660–670, Sep. 2018.
- [33] C. E. Jones *et al.*, "A novel methodology for macro-scale, thermal characterization of carbon fiber-reinforced polymer for integrated aircraft electrical power systems," *IEEE Trans. Transport. Electric.*, vol. 5, no. 2, pp. 479–489, Jun. 2019.
- [34] C. E. Jones *et al.*, "A route to sustainable aviation: A roadmap for the realization of aircraft components with electrical and structural multifunctionality," *IEEE Trans. Transport. Electric.*, vol. 7, no. 4, pp. 3032–3049, Dec. 2021.
- [35] S. Wang, S. Zhang, and S. Ma, "An energy efficiency optimization method for fixed pitch propeller electric aircraft propulsion systems," *IEEE Access*, vol. 7, pp. 159986–159993, 2019.
- [36] S. Ma, S. Wang, C. Zhang, and S. Zhang, "A method to improve the efficiency of an electric aircraft propulsion system," *Energy*, vol. 140, pp. 436–443, Dec. 2017.
- [37] A. Misra, "Energy storage for electrified aircraft: The need for better batteries, fuel cells, and supercapacitors," *IEEE Electr. Mag.*, vol. 6, no. 3, pp. 54–61, Sep. 2018.
- [38] A. R. Gnad, R. L. Speth, J. S. Sabnis, and S. R. H. Barrett, "Technical and environmental assessment of all-electric 180-passenger commercial aircraft," *Prog. Aerosp. Sci.*, vol. 105, pp. 1–30, Feb. 2019.
- [39] Chevrolet. (2016). *2016 Chevrolet Volt Battery System*. [Online]. Available: https://media.gm.com/content/dam/Media/microsites/product/Volt_2016/doc/VOLT_BATTERY.pdf
- [40] J. J. Lamb and O. S. Burheim, "Lithium-ion capacitors: A review of design and active materials," *Energies*, vol. 14, no. 4, p. 979, Feb. 2021.
- [41] L. Spitthoff, P. R. Shearing, and O. S. Burheim, "Temperature, ageing and thermal management of lithium-ion batteries," *Energies*, vol. 14, no. 5, p. 1248, Feb. 2021.
- [42] L. Spitthoff *et al.*, "Thermal management of lithium-ion batteries," in *Micro-Optics and Energy*. Berlin, Germany: Springer, 2020, pp. 183–194.
- [43] M. S. Wahl, L. Spitthoff, H. I. Muri, A. Jinasena, O. S. Burheim, and J. J. Lamb, "The importance of optical fibres for internal temperature sensing in lithium-ion batteries during operation," *Energies*, vol. 14, no. 12, p. 3617, Jun. 2021.
- [44] X. Feng, M. Ouyang, X. Liu, L. Lu, Y. Xia, and X. He, "Thermal runaway mechanism of lithium ion battery for electric vehicles: A review," *Energy Storage Mater.*, vol. 10, pp. 246–267, Jan. 2018.
- [45] J. Kim, J. Oh, and H. Lee, "Review on battery thermal management system for electric vehicles," *Appl. Thermal Eng.*, vol. 149, pp. 192–212, Feb. 2019.
- [46] C. Pernet *et al.*, "Methodology for sizing and performance assessment of hybrid energy aircraft," *J. Aircr.*, vol. 52, no. 1, pp. 341–352, Jan. 2015.



Trym Bærheim received the M.Sc. degree in mechanical engineering from the Norwegian University of Science and Technology, Trondheim, Norway, in 2021.

He is currently a Component Design Engineer with Rolls-Royce Electrical Norway, Trondheim, where he is building, designing, and testing electric engines for next-generation aircraft.



Jonas Kristiansen Nøland (Senior Member, IEEE) was born in Drammen, Norway, in 1988. He received the M.Sc. degree in electric power engineering from the Chalmers University of Technology, Gothenburg, Sweden, in 2013, and the Ph.D. degree in engineering physics from Uppsala University, Uppsala, Sweden, in 2017.

Since 2018, he has been an Associate Professor with the Department of Electric Power Engineering, Norwegian University of Science and Technology, Trondheim, Norway. His current research interests include excitation systems, improved utilization of electrical machines, high-power machinery for aircraft applications, hyperloop propulsion and levitation, and transportation electrification in general.

Dr. Nøland also serves as an Editor for the IEEE TRANSACTIONS ON ENERGY CONVERSION and an Associate Editor for the IEEE TRANSACTIONS ON INDUSTRIAL ELECTRONICS.



Jacob J. Lamb is currently an Early Career Associate Professor of energy and process technology with the Norwegian University of Science and Technology, Trondheim, Norway. He is involved with Norwegian and European projects aiming to advance the field of energy storage and conversion, with his main focus on digitalization methods.



Odne S. Burheim is currently with the Norwegian University of Science and Technology (NTNU), Trondheim, Norway, where he specializes in processes of e-fuels and energy storage. He is also a Group Leader of the Sustainable Energy Research Group, Department of Energy and Process Engineering, NTNU.

He works in the fields of battery manufacturing, aging, and heat management. He also works in the fields of hydrogen production, biofuel production, and salinity gradient energy systems. He is the author of the book *Engineering Energy Storage* and has published more than 100 peer reviewed research papers in these fields.